

Study of PN-code Capture Method with High Dynamic and Low SNR in Near Space

Ke Sun *, Xiaomin Hou, Qiang Zhao

Equipment Academy, Beijing, China

Email: 15201500878@126.com; 13801244993@139.com; zqaniu@163.com

* Corresponding Author

Abstract—Considering the requirement of building near space tt&c system, it designed a parallel PN-code capture method based on FFT. First, it gave a clear derivation of the principle of parallel PN-code capture method, analyzed the capture performance in detail, and finally proved the feasibility of the method through simulation experiment. This method on the one hand weakens the influence of the doppler frequency, and reduces the capture dimension from 2 to 1. At the same time, it achieved the related operations, the relative value of local code and receiving yards was acquired. By this, some special requirements were satisfied and the circuit was simplified, capture speed was improved very much. On the whole, the method overcomes the poor performance under low SNR of traditional capture method, has a good prospect of engineering application.

Keywords-Near Space; FFT; PN-code Capture; High Dynamic; Low SNR

I. INTRODUCTION

Near space is at an altitude of 20 km to 100 km in space area between the satellite platform and aviation platform, which is the must-go to outer space. At the same time, it is a strategic space for human to develop. As a new research field, many of the techniques need to be innovative designed, including the measurement & control and information transmission system. Scientific research institutions at home and abroad had already started the study of tt&c system in near space because it has a series of advantages: Low cost, rapid deployment, less ground equipment, flexible use and easy recycling^[1].

There are 16068 patents about spread spectrum in National Patent Office of America, further involving PN-code capture is 590. These patents contain design, synchronization, sending, receiving and positioning of PN-code, etc^{[2]-[4]}. In the domestic, Tsinghua university, Shanghai Jiaotong University and Beijing University of Aeronautics and Astronautics and Aerospace Science and Technology Group etc have made a series of innovative research results. In the satellite signal capturing and tracking algorithm^[5].

Because of the complexity of communication environment in near space, high-speed movement of communication carrier causes the influence of PN-code phase delay to wireless mobile communication been enhanced. Therefore, the communication system can work effectively and reliably or not, to a large extent depends on the presence of PN-code capture system^{[6][7]}. At the same

time, considering the tt&c platforms must possess information security protection, such as anti-interference, resistance to intercept, secret transmission^[8], this article using signal modulation system of direct spread spectrum, and design a PN-code capture method based on FFT. Most of traditional PN-code capture methods are based on slide correlation and matched filtering. This method not only overcomes the poor capture performance under low SNR of traditional methods, but also can greatly reduce the average capture time.

II. PRINCIPLE OF PARALLEL PN-CODE CAPTURE METHOD BASED ON FFT

The parallel PN-code capture method based on FFT take advantages of FFT skillfully, compensating the carrier phase offset of received signal caused by doppler frequency through parallelly. It increases adaptation range to doppler frequency greatly and reduce the capture dimension from 2 to 1 so that the PN-code capture time is shortened exponentially.

The principle of parallel PN-code capture method based on FFT is as follows: The cycle of received PN-code is divided into a number of equal length periods, accordingly, the local code id divided into the same number periods, then do the related operations of received codes and local codes in each period and send the result to FFT processing unit. As shown in Fig. 1.

FFT is actually a process of Weighted accumulation for each input signal, and weighted and can be seen as the process of phase shift for input signal^[9]. With the doppler frequency, the output of two adjacent part-correlators has a certain phase difference which can be eliminated completely or partly through FFT operation. When the local code and receiving code are synchronous, if the compensated phase of k ($k \in (0, 1, 2, \dots, D-1)$) road was nearest to the phase difference above mentioned, this branch has the largest output value. However, FFT cannot eliminate the influence of different part-correlators' output caused by doppler frequency.

In Fig. 1, useful signal and noise of input are independent of each other, and the process is linear from A/D sample to D points FFT operation, so useful signal and noise can be taken into account separated. Input signal $r(t) = s(t) + n(t)$, $s(t)$ is the useful signal and $n(t)$ is the noise.

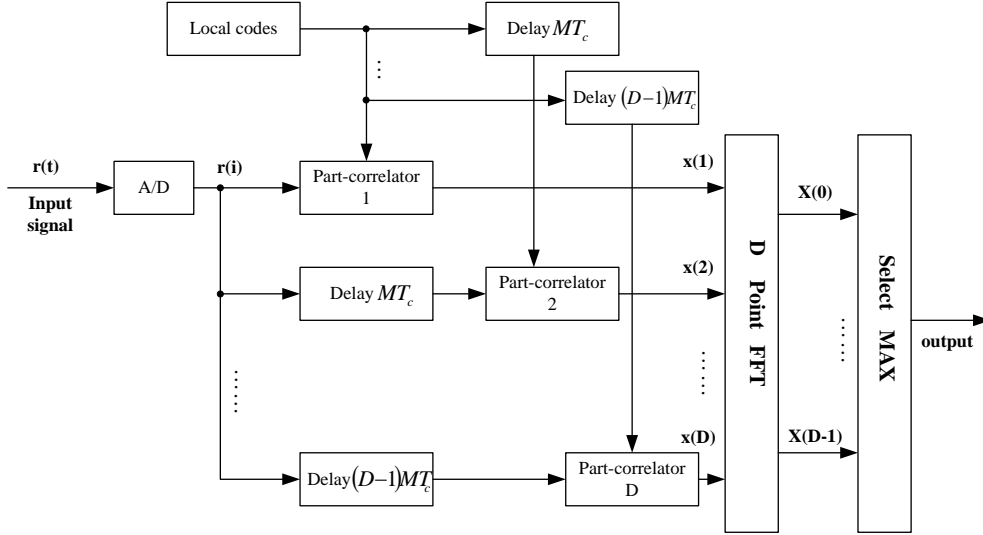


Figure 1. Schematic of PN-code capture method based on FFT

Assuming that the received useful signal $s(t)$ had been down-converted to zero intermediate frequency, but doppler frequency f_d still remained and it has a unit amplitude. In order to more easily analyze the influence doppler frequency to peak of coherent accumulation, it just discuss the case that local PN-codes and received PN-codes are synchronous.

$$s(t) = PN(t)e^{j(2\pi f_d t + \phi)} \quad (1)$$

$PN(t)$ is the received PN-codes, if width of PN-codes is T_c , and length of PN-codes is N , sampling $s(t)$ with a interval T_c , it can get:

$$s(i) = PN(i)e^{j(2\pi f_d T_c i + \phi)} \quad (2)$$

Assuming that the Noise component $n(t)$ in $r(t)$ is Narrowband and smoothly white gaussian noise and bandwidth is $2B$ (B is code rate of spread spectrum, $B = \frac{1}{T_c}$), density of bilateral power spectral is $N_0/2$, mean value is 0 , variance is $\sigma^2 = N_0 B$.

$n(t)$ can be written as:

$$n(t) = n_c(t) \cos[2\pi(f_c + f_d)t] + n_s(t) \sin[2\pi(f_c + f_d)t] \quad (3)$$

$f_c + f_d$: carrier frequency of received signal; f_c : carrier frequency of transmitted signal; f_d : doppler frequency.

Bandwidth, bilateral power spectral, mean value and variance of $n_c(t)$, $n_s(t)$ and $n(t)$ are all equal, respectively are $2B$, $N_0/2$, 0 , σ^2 .

Assuming that $n(t)$ was divided into two branches, and respectively mix frequency with inphase signal and quadrature signal (frequency is f_c) that come from local oscillator, through low pass filter can get it:

$$q_n(t) = n_c(t) \cos(2\pi f_d t) + n_s(t) \sin(2\pi f_d t) \quad (4)$$

$$i_n(t) = -n_c(t) \sin(2\pi f_d t) + n_s(t) \cos(2\pi f_d t) \quad (5)$$

Set up the sample rate equal to code rate as B . After sampling $q_n(t)$, $i_n(t)$, it get that:

$$q_n(k) = n_c(k) \cos(2\pi f_d T_c k) + n_s(k) \sin(2\pi f_d T_c k) \quad (6)$$

$$i_n(k) = -n_c(k) \sin(2\pi f_d T_c k) + n_s(k) \cos(2\pi f_d T_c k) \quad (7)$$

The output of correlation operation between $i_n(k)$, $q_n(k)$ and local code is I_n , Q_n :

$$Q_n = \frac{1}{N} \sum_{k=1}^N PN(k-p) \cdot [n_c(k) \cos(2\pi f_d T_c k) + n_s(k) \sin(2\pi f_d T_c k)] \quad (8)$$

$$I_n = \frac{1}{N} \sum_{k=1}^N PN(k-p) \cdot [-n_c(k) \sin(2\pi f_d T_c k) + n_s(k) \cos(2\pi f_d T_c k)] \quad (9)$$

For the band-limited white noise with the bandwidth of $2B$, the random from sampling with a sample rate B are independent of each other. At the same time $PN(k)$ ($PN(k) = \pm 1$) and $n(k)$ are independent of each other, so the mean value and variance are:

$$\begin{aligned} E[Q_n] &= E\left[\frac{1}{N} \sum_{k=1}^N PN(k-p) [n_c(k) \cos(2\pi f_d T_c k) + n_s(k) \sin(2\pi f_d T_c k)]\right] \\ &= \frac{1}{N} \sum_{k=1}^N \{E[PN(k-p)] \cdot E[n_c(k)] \cdot E[\cos(2\pi f_d T_c k)]\} \\ &\quad + \frac{1}{N} \sum_{k=1}^N \{E[PN(k-p)] \cdot E[n_s(k)] \cdot E[\sin(2\pi f_d T_c k)]\} \\ &= 0 \end{aligned} \quad (10)$$

Similarly, $E[I_n] = 0$.

$$\begin{aligned} D[Q_n] &= D\left[\frac{1}{N} \sum_{k=1}^N PN(k-p) [n_c(k) \cos(2\pi f_d T_c k) + n_s(k) \sin(2\pi f_d T_c k)]\right] \\ &= \frac{1}{N^2} \sum_{k=1}^N \{D[PN(k-p) \cdot n_c(k) \cdot \cos(2\pi f_d T_c k)]\} \\ &\quad + \frac{1}{N^2} \sum_{k=1}^N \{D[PN(k-p) \cdot n_s(k) \cdot \sin(2\pi f_d T_c k)]\} \\ &= \frac{\sigma^2}{N} \end{aligned} \quad (11)$$

Similarly, $D[I_n] = \frac{\sigma^2}{N}$.

From what has been discussed above, the statistical property of noise output from accumulator has nothing to do with the carrier frequency doppler.

In conclusion, the noise output from every correlator is Gaussian noise, and its mean value equal to 0, variance is $\frac{\sigma^2}{M}$; The output noise of k point normalized FFT : mean value=0, variance= $\frac{\sigma^2}{N}$.

III. ANALYSIS OF PN-CODE CAPTURE PERFORMANCE

The input signal of capture circuit is $r(t) = s(t) + n(t)$, thereinto, the useful signal is $s(t) = \sqrt{2P} \cdot PN(t) \cdot e^{j(2\pi(f_d + f_c)t + \phi)}$, its power is P . $n(t)$ is noise, the mean value of it is 0, variance is σ^2 , input SNR is $SNR = P/\sigma^2$.

Assuming there were just two branches, z is the input signal of threshold judgment unit of capture circuit:

$$z = \sqrt{I^2 + Q^2} = \sqrt{[I_s(p, f_d) + I_n]^2 + [Q_s(p, f_d) + Q_n]^2} \quad (12)$$

I_n, Q_n can be acquired from the formula (8) and (9). $I_s(p, f_d), Q_s(p, f_d)$ are useful signal acquired from Coherent accumulation between In-phase branch and Quadrature branch. And

$$I_s^2(p, f_d) + Q_s^2(p, f_d) = 2P \cdot R_{PN}^2(p) \cdot \frac{\sin^2(\pi f_d T)}{N^2 \sin^2(\pi f_d T_c)}$$

Letting $I_s^2(p, f_d) + Q_s^2(p, f_d) = A^2$, when $A=0$, z obey Rayleigh distribution $p_{Rayleigh}(z)$:

$$p_{Rayleigh}(z) = \frac{z}{\delta^2} \exp\left(-\frac{z^2}{2\delta^2}\right) \quad z \geq 0 \quad (13)$$

When $A \neq 0$, z obey the generalized Rayleigh distribution (Rice distribution) $p_{Ricean}(z)$:

$$p_{Ricean}(z) = \frac{z}{\delta^2} \exp\left[-\frac{z^2 + A^2}{2\delta^2}\right] I_0\left(\frac{Az}{\delta^2}\right) \quad z \geq 0 \quad (14)$$

Thereinto, $I_0(\cdot)$ is the first kind of zero order modified Bessel function. Detailed analysis of the above conclusion is in references^[10].

Assuming that:

H_0 -local codes and received codes were not synchronous and phase offset is greater than or equal to an element, at this time $A=0$.

H_1 -local codes and received codes were basically synchronous and phase offset is less than or equal to an element, at this time $A>0$.

1. False alarm probability P_{fa}

V_T is judgment threshold, then the normalized judgment threshold is $\frac{V_T}{\delta}$. When local codes and received codes are not synchronous, D output of FFT are independent of each other, and even if one of them is greater than the threshold, false alarm will appear.

$$\begin{aligned} P_{fa} &= 1 - \left[1 - P(H_1/H_0)\right]^D = 1 - \left[1 - \int_{V_T}^{+\infty} p_{Rayleigh}(z) dz\right]^D \\ &= 1 - \left[1 - \int_{V_T}^{+\infty} \frac{z}{\delta^2} e^{-\frac{z^2}{2\delta^2}} dz\right]^D = 1 - \left[1 - e^{-\frac{1}{2}\left(\frac{V_T}{\delta}\right)^2}\right]^D \end{aligned} \quad (15)$$

Setting threshold on the basis of constant false alarm probability:

$$V_T = \delta \sqrt{-2\ln(1 - \sqrt[D]{1 - P_{fa}})} \quad (16)$$

2. Detection probability and missed detection probability

Writing the k th output that greater than threshold of FFT as $P_d(k)$, the detection probability is:

$$\begin{aligned} P_d(k) &= P(H_1/H_1) = \int_{V_T}^{+\infty} p_{Ricean}(z) dz \\ &= \int_{V_T}^{+\infty} \frac{z}{\delta^2} \exp\left[-\frac{z^2 + A(k)^2}{2\delta^2}\right] I_0\left(\frac{A(k)z}{\delta^2}\right) dz \end{aligned} \quad (17)$$

When local codes and received codes are synchronous, missed will appear just in the case that none of D output is greater than threshold. Therefore, missed detection probability $P_{om}(k)$ is:

$$P_{om}(k) = \prod_{k=0}^{D-1} P(H_0/H_1) = \prod_{k=0}^{D-1} \int_0^{V_T} p_{Ricean}(z) dz = \prod_{k=0}^{D-1} (1 - P_d(k)) \quad (18)$$

According to the definition of the Q function, $Q(\alpha, \beta) = \int_{\beta}^{+\infty} t I_0(\alpha t) \exp[-(t^2 + \alpha^2)/2] dt$ from transform of formula (17), it can get:

$$\begin{aligned} P_d(k) &= \int_{\frac{V_T}{\delta}}^{+\infty} \frac{z}{\delta} \exp\left[-\frac{\left(\frac{z}{\delta}\right)^2 + \left(\frac{A(k)}{\delta}\right)^2}{2}\right] I_0\left(\frac{A(k)}{\delta} \cdot \frac{z}{\delta}\right) d\left(\frac{z}{\delta}\right) \\ &= Q\left(\frac{A(k)}{\delta}, \frac{V_T}{\delta}\right) = Q\left(\frac{A(k)}{\delta}, \sqrt{-2\ln(1 - \sqrt[D]{1 - P_{fa}})}\right) \end{aligned} \quad (19)$$

3. Mean capture time of PN-code

For the single PN-code capture mode, mean capture time of PN-code T_{acq} decide by detection probability P_d , false alarm probability P_{fa} , price factor of false alarm K , code unit number to be searched q , and time of single post integration T .

$$T_{acq} = \frac{(2 - P_d)(1 + KP_{fa})}{2P_d} qT \quad (20)$$

IV. ANALYSIS OF CAPTURE RESULTS OF SIMULATION

According to engineering practice, set the change range of f_d -100kHz to +100kHz, and f_d' is $\pm 3kHz$. After the change range of doppler frequency is divided into several equal parts, scanning on every part in turn and capturing the PN-code, at last comparing the results of coherent accumulation with the threshold and making the judgment.

1. Adopting the m sequence as the PN-code, length is 511, code rate is 500kHz; Setting sampling rate 1000kHz,

sample points in one period $N=1023$; length of part-correlator $M=1$, FFT operation points $D=1024$; power of signal $P=1/2$, power of noise $\sigma^2=0.5 \times 10^{-\left(\frac{SNR}{10}\right)}$.

2. Setting interval of doppler frequency $\frac{1}{T} \approx 1kHz$,

200 capture channels are needed in total.

3. Integration time: a period of PN-code,

$$T = \frac{1}{500k} \times 511 = 1.022ms \approx 1ms.$$

4. Set of threshold: according to constant false alarm probability, threshold V_T is:

$$V_T = \frac{\sigma}{\sqrt{N}} \sqrt{-2 \ln(1 - 10^{24} \sqrt{1 - P_{fa}})} = \frac{\sigma}{\sqrt{1023}} \sqrt{-2 \ln(1 - 10^{24} \sqrt{1 - P_{fa}})} \quad (21)$$

5. Detection probability:

Amplitude of the input useful signal of threshold judgment unit:

$$A(k) = \sqrt{I_s^2(p, f_d) + Q_s^2(p, f_d)} = \left| \sqrt{2P} \cdot R_{PN}(p) \cdot \frac{\sin(\pi f_d N T_c)}{N \sin(\pi f_d T_c)} \right| \quad (22)$$

In the case that performance of carrier capture is the most poor, $f_d = \pm \frac{1kHz}{2} = \pm 500Hz$, at this time,

$\left| \frac{\sin(\pi f_d T)}{N \sin(\pi f_d T_c)} \right| \approx 0.31$. Plugging $A = 0.31 \sqrt{2P} = 0.31$, $d = \frac{\sigma}{\sqrt{1022}}$ in formula (19), the detection probability can be gotten:

$$P_d = Q \left[\frac{A}{\delta}, \frac{V_T}{\delta} \right] = Q \left[22.6 \sqrt{\frac{P}{\sigma^2}}, \sqrt{-2 \ln(1 - \sqrt{1 - P_{fa}})} \right] \quad (23)$$

$$= Q \left[22.6 \sqrt{SNR}, \sqrt{-2 \ln(1 - \sqrt{1 - P_{fa}})} \right]$$

A. Detection of correlation peak of different FFT output branches

Checking if there is a correlation peak of FFT output or not. For different branches, when local PN-codes and input PN-codes are synchronous, there will be a correlation peak, and the peak value is the max value. At the same time, correlation peak will not appear in other branches, as shown in Fig. 2.

From Fig. 2, the method based on FFT can detect the difference of synchronous element when correlation peak appears, but correlation peak can just be detected in valid branches.

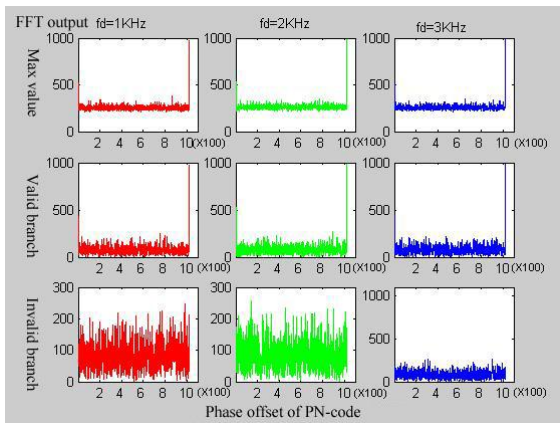


Figure 2. correlation peak of different FFT output branches

B. Relationship between detection probability and SNR under different false alarm probability

When doppler frequency $f_d=1kHz$, relationship between detection probability and SNR under different false alarm probability shown as Fig. 3. In the figure, scatter points are the simulation results, and the solid line is the theoretical results, they two fit very well. The value of false alarm probability respectively is 10^{-1} , 10^{-2} , 10^{-3} , 10^{-4} , 10^{-5} , 10^{-6} , the corresponding detection probability results are from top to bottom.

From Fig. 3, detection probability P_d decreases with the decrease of the false alarm probability P_{fa} , and when the SNR decreases gradually, detection probability will be close to false alarm probability, in limit case, they are equal to each other. Detection probability P_d increases with the increase of the false alarm probability P_{fa} , and when the SNR reaches a certain value, no matter how to set threshold, detection probability tend to be 1. Under the simulation conditions, when $SNR > -15dB$, no matter how other parameters be set, PN-code can always be captured quickly and exactly. In following simulations, in order to analyze the influence that threshold and remaining doppler frequency to performance of PN-code capture, SNR is set lower properly, adopted $-20dB$.

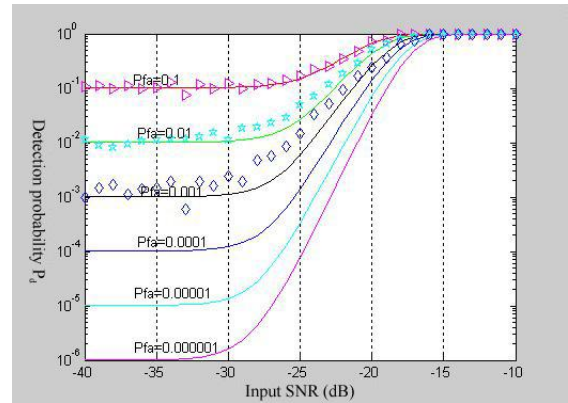


Figure 3. Theoretical curves and simulation results of detection probability and SNR under different false alarm probability ($f_d=1kHz$)

C. Relationships between detection probability and mean capture time as well as doppler frequency under different false alarm probability

When $SNR=-20dB$, relationship between different detection probability P_d , mean capture time T_{acq} and doppler frequency f_d shown as Fig. 4 and Fig. 5.

In the figure, scatter points are the simulation results, and the solid line is the theoretical results, they two fit very well. The value of false alarm probability respectively is 10^{-1} , 10^{-2} , 10^{-3} , 10^{-4} , 10^{-5} , 10^{-6} , the corresponding detection probability results are from top to bottom.

From Fig. 4, when $SNR=-20dB$, detection probability P_d decreases with the decrease of the false alarm probability P_{fa} , detection probability P_d changes periodically with the change of doppler frequency, in detail: when f_d is equal to $-1000Hz$, $0Hz$, $1000Hz$,

value of P_d will be max, and when f_d is equal to -500Hz , 500Hz , value of P_d will be min. The reason is as following: from formula (19), the resolution of FFT to doppler frequency is 1KHz in the simulation, when the f_d is equal to integer times of 1KHz , The compensation of FFT can eliminate the influence of doppler frequency absolutely. And when the f_d is not equal to integer times of 1KHz , but equal to integer times of $1/2\text{KHz}$, there will still remaining a max doppler frequency equal to 500Hz , at this time, the detection probability will be minimum. The simulation results are consistent with theoretical analysis.

From Fig. 5, when $\text{SNR}=-20\text{dB}$, mean capture time T_{acq} increases with the decrease of the false alarm probability P_{fa} and changes periodically with the change of doppler frequency, the period is 1KHz . If doppler frequency was compensated fully, when P_{fa} is set as 10^{-1} , T_{acq} is 1.2s . When P_{fa} is set as 10^{-4} , T_{acq} is 6.8s . And if there exiting a 500Hz doppler frequency, when P_{fa} is set as 0.1 , T_{acq} is 3.9s ; when P_{fa} is set as 10^{-4} , T_{acq} is 138s .

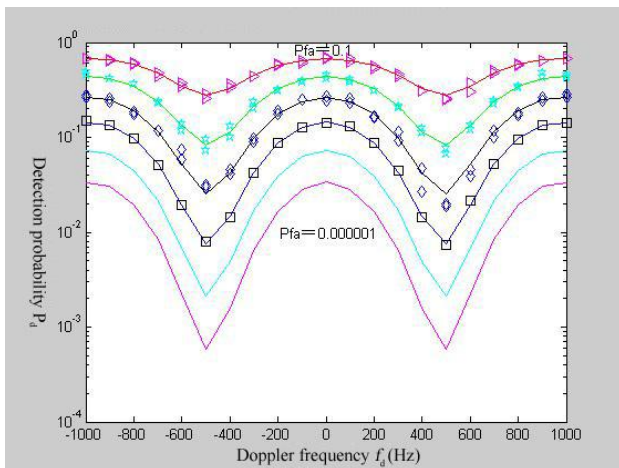


Figure 4. Theoretical curves and simulation results of detection probability and doppler frequency under different false alarm probability($\text{SNR}=-20\text{dB}$)

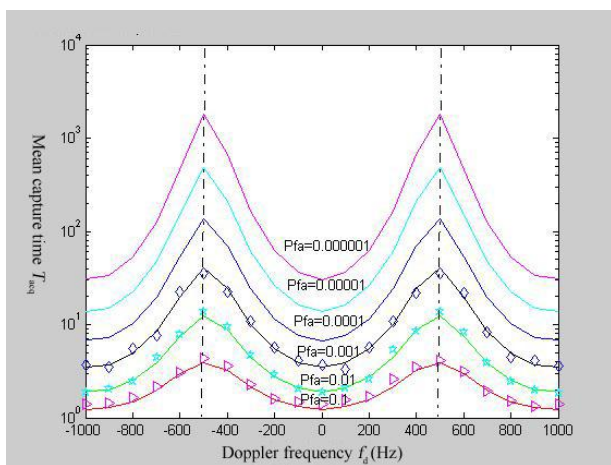


Figure 5. Theoretical curves and simulation results of mean capture time and doppler frequency under different false alarm probability($\text{SNR}=-20\text{dB}$)

D. Relationships between detection probability and mean capture time as well as doppler frequency under different SNR

When P_{fa} is set as 10^{-4} , the relationships between detection probability and mean capture time as well as doppler frequency under different SNR are shown as Fig. 6 and Fig. 7.

In the figures, scatter points are the simulation results, and the solid lines are the theoretical results; SNR is set as: -12dB , -15dB , -18dB , -21dB , -24dB and -27dB , the corresponding detection probability results are from top to bottom and the corresponding mean capture times are from bottom to top.

From Fig. 6 and Fig. 7, when $\text{SNR}=-12\text{dB}$, $\text{SNR}=-15\text{dB}$, $\text{SNR}=-18\text{dB}$, simulation results are close to theoretical curves; when $\text{SNR}=-21\text{dB}$, difference between simulation results and theoretical curves appears; when $\text{SNR}=-12\text{dB}$, $\text{SNR}=-15\text{dB}$, simulation results is far from theoretical curves. It proves that the critical value of SNR is about 20dB which is fit to the analysis above.

In addition, when $\text{SNR} > -21\text{dB}$ and decreases linearly, the corresponding detection probability decreases obey a approximately exponential rule. Furthermore, detection probability changes periodically with the change of doppler frequency proves that the resolution of doppler frequency is 1KHz .

Magnifying the Fig. 7 partly, when false alarm probability P_{fa} is 10^{-4} , capture time under different SNR is:

If $\text{SNR}=-12\text{dB}$, T_{acq} is 0.52s ;

If $\text{SNR}=-15\text{dB}$, when f_d is set as 0 , T_{acq} is 0.52s ;
when f_d is set as 500Hz , T_{acq} is 1.4s ;

If $\text{SNR}=-18\text{dB}$, when f_d is set as 0 , T_{acq} is 1.4s ;
when f_d is set as 500Hz , T_{acq} is 19.7s ;

It proves further more: when $\text{SNR} > -15\text{dB}$, the performance of PN-code capture is more reliable and stable.

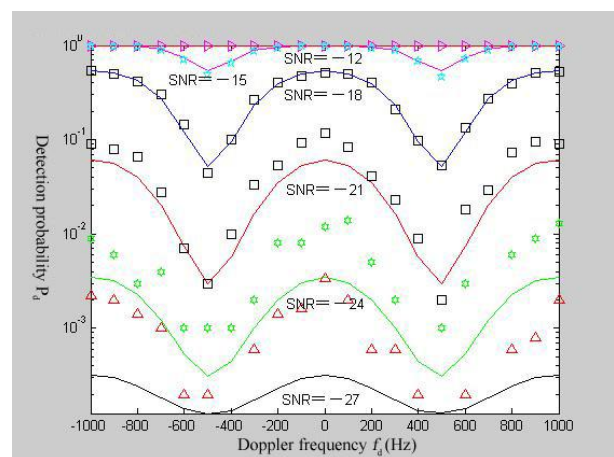


Figure 6. Theoretical curves and simulation results of detection probability and doppler frequency under different SNR ($P_{fa} = 10^{-4}$)

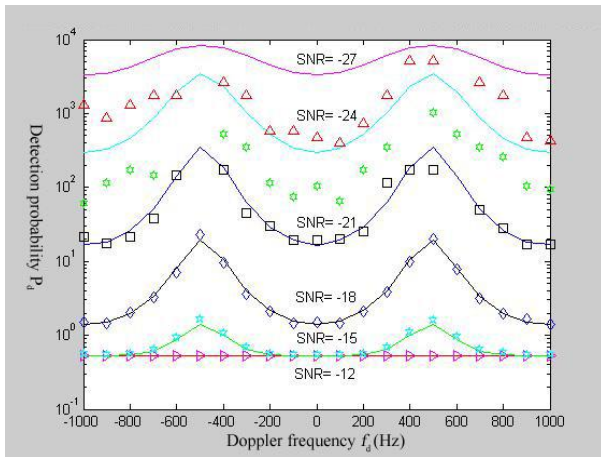


Figure 7. Theoretical curves and simulation results of mean capture times and doppler frequency under different false alarm probability ($P_{fa} = 10^{-4}$)

V. CONCLUSIONS

With the further development of wireless communication, as one important branch of communication network, near space communication is attracting more and more attention. According to the character that high information rate and high dynamic, it emphatically analyzes the PN-code capture method based on FFT. The method not only weakened the influence of doppler frequency but also finished the correlation synchronously.

According to the analysis and simulations above, conclusions can be gotten as following:

1. In simulations, set the number of correlator as 1023, and the length of every correlator as 1, point of FFT as 1024, when SNR=-15dB, no matter how threshold is set, PN-code can be captured in about 0.5s.

2. Under the simulation condition, the resolution of doppler frequency is 1kHz. When the doppler frequency is equal to integer times of 1kHz, The doppler frequency can be eliminated absolutely. And when the doppler frequency is equal to odd times of 1/2 kHz, there will remaining a

max doppler frequency equal to 500Hz, the correlation peak will decrease 2 dB.

3. This method is fit to doppler frequency very well, can satisfy the need of PN-code capture in high dynamic condition (including high doppler frequency and high change rate of doppler frequency).

4. This method can satisfy the need of measurement and control platform in near space.

From what has been discussed above, benefiting from the development of DSP, FFT can be completed easily and the speed of it is higher and higher. Therefore, it is a good choice to adopt the method based on FFT to capture PN-code.

REFERENCE

- [1] X. M. Guan. "Implementation of carrier acquisition and track in HDHI situation in near space," Journal of Sichuan university (Engineering science edition), vol. 41(5), pp.30-35, 2009.
- [2] Miura R, Suzuki M. "Preliminary flight test program on telecom and broadcasting using high altitude platform stations," Wireless Personal Communications, vol. 24(1), pp.341-361, 2003.
- [3] Thomson J, Grace D, Capstick M H. "Optimizing an array of antennas for cellular coverage from high altitude platform," IEEE Transactions on Wireless Communications, vol. 2(3), pp. 168-175, 2003.
- [4] Cianca E, Prasad R. "De Sanctis Integrated satellite-HAP systems," IEEE Transaction on Communications Magazine, vol. 43(12), pp. 33-39, 2005.
- [5] Y. M. Ren. "The research of modulation technology on near space tt&c communication system and its simulation," Xi'an: Academic, Xi'an university of electronic science and technology, 2011.
- [6] Lacky R, Upmal J, Speakeasy D W. "The military software radio," IEEE Communications Magazines, pp. 2023-2027, May 1995.
- [7] S. Y. T, R. C. Wu. "Frequency acquisition and tracking in high dynamic environments," IEEE Transactions on Vehicular Technology, vol. 49(6), pp. 2419-2429, 2006.
- [8] F. Min. "Research on the acquisition and tracking of the high dynamic tt&c signal in near space," Xi'an: Academic, Xi'an university of electronic science and technology, 2012.
- [9] W. Yuan. "The design of high speed near space vehicle tt&c link and simulation platform implementation," Xi'an: Academic, Xi'an university of electronic science and technology, 2012.
- [10] C. X. Fan, D. Y Lu. Communication theory (The fourth edition). Peking: National defence industry press, 1992.